

Dynamical critical exponent of the Jaynes-Cummings-Hubbard model

M. Hohenadler,¹ M. Aichhorn,² S. Schmidt,³ and L. Pollet³

¹*Institut für Theoretische Physik und Astrophysik, Universität Würzburg, 97074 Würzburg, Germany*

²*Institut für Theoretische Physik – Computational Physics, TU Graz, 8010 Graz, Austria*

³*Institut für Theoretische Physik, ETH Zurich, 8093 Zürich, Switzerland*

(Dated: May 24, 2022)

An array of high- Q electromagnetic resonators coupled to qubits gives rise to the Jaynes-Cummings-Hubbard model describing a superfluid to Mott insulator transition of lattice polaritons. From mean-field and strong coupling expansions, the critical properties of the model are expected to be identical to the scalar Bose-Hubbard model. A recent Monte Carlo study of the superfluid density on the square lattice suggested that this does not hold for the fixed-density transition through the Mott lobe tip. Instead, mean-field behavior with a dynamical critical exponent $z = 2$ was found. We perform large-scale quantum Monte Carlo simulations to investigate the critical behavior of the superfluid density and the compressibility. We find $z = 1$ at the tip of the insulating lobe. Hence the transition falls in the 3D XY universality class, analogous to the Bose-Hubbard model.

PACS numbers: 71.36.+c, 73.43.Nq, 78.20.Bh, 42.50.Ct

Introduction A remarkable success of theoretical physics is the development of a theory of phase transitions which provides a unified description of apparently distinct systems in terms of a few different universality classes characterized by universal critical exponents. The universality of a transition is completely determined by the dimension of the system, the order parameter and the range of interactions. An interesting example is the Mott insulator to superfluid (MI-SF) transition of lattice bosons, first studied in the framework of the Bose-Hubbard model (BHM) [1]. When driven by density fluctuations, the MI-SF transition is known to be in the universality class of the dilute Bose gas with a dynamical critical exponent $z = 2$ [1, 2]. However, when the density of bosons is kept fixed during the transition its universality class changes and corresponds to the (2+1)D XY model with $z = 1$ [1, 3, 4].

The experimental realization of the BHM with ultra-cold atoms in optical lattices [5] nearly a decade ago has opened up a fast growing and versatile field of condensed matter physics. More recently, the realization of Bose-Einstein condensation of weakly interacting polaritons, i.e., quasiparticles that form when light strongly interacts with matter, in high- Q cavities [6] has triggered an immense interest in realizing condensed matter systems with photonic systems. A recent theoretical focus has been on the MI-SF transition of polaritons [7–16]. The Jaynes-Cummings-Hubbard model (JCHM) has been introduced to describe such a quantum phase transition of light in an array of coupled quantum electrodynamics (QED) cavities, each containing a single photonic mode interacting with a two-level system (qubit) [7–9]. The competition between strong photon-qubit coupling, giving rise to an effective photonic repulsion (localization), and the photon hopping between cavities (delocalization) leads to a phase diagram featuring Mott lobes reminiscent of those of ultracold atoms in optical lattices as described by the BHM. The realization of the JCHM has been proposed in various solid-state or quantum-optical systems, e.g., with nitrogen-vacancy (NV) centers in diamond [7–9], quantum dot excitons [17], superconducting qubits [13] and trapped ions [18]. Device integration, high tunability and individual addressability of each cavity make wide parameter regimes easily accessible. Cavity or

circuit QED arrays thus constitute one of the most promising architectures for quantum information processing and offer the possibility to study fundamental questions of interacting quantum systems. For a recent review of many-body physics in coupled-cavity arrays see Ref. [19].

The phase diagram and excitation spectra of the JCHM have been accurately determined by analytical [7, 13–15] as well as numerical methods [8–12, 16, 20]. However, an intriguing open question concerns the universality class of the fixed-density transition of the JCHM. Quantum Monte Carlo (QMC) calculations of the superfluid density [12] suggest that the universality class at the tip of the Mott lobe of the JCHM is different (namely mean-field like) from the BHM. On the contrary, strong-coupling expansion [14, 15] and an effective action approach [13] show that the same critical theory applies to both models. The discrepancy with the QMC predictions is very surprising, especially since the analytical arguments for arriving at a critical theory are similar to the BHM and are well understood. One would therefore expect the same scaling behavior, e.g., of the superfluid density, for the BHM and the JCHM.

In this Rapid Communication we resolve the controversy between analytical and numerical findings and present results from extensive QMC simulations on the two-dimensional (2D) square lattice. We go beyond previous studies in two significant ways: (i) by using much larger system sizes, and (ii) by studying both the superfluid density and the compressibility.

Model The JCHM is defined by the Hamiltonian

$$H = \sum_i h_i^{\text{JC}} - t \sum_{\langle ij \rangle} (a_i^\dagger a_j + \text{H.c.}) - \mu \hat{N}, \quad (1)$$

with the JC Hamiltonian for site i [21]

$$h_i^{\text{JC}} = \omega_p a_i^\dagger a_i + \omega_q \sigma_i^+ \sigma_i^- + g \left(\sigma_i^+ a_i + \sigma_i^- a_i^\dagger \right),$$

and the total number of polaritons $\hat{N} = \sum_i (a_i^\dagger a_i + \sigma_i^+ \sigma_i^-)$ (combined number of photons and qubit excitations), which is a conserved quantity and can be controlled via the chemical

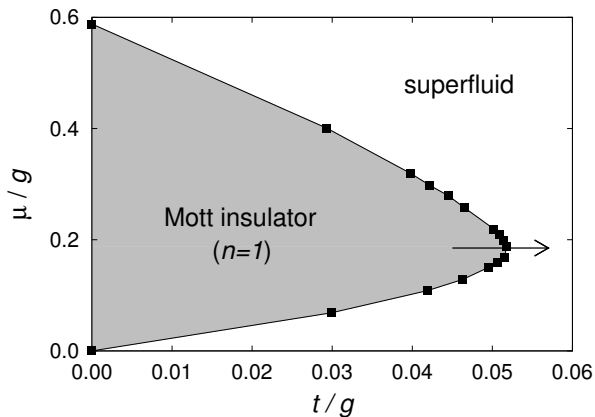


FIG. 1: Phase diagram of the JCHM with zero detuning on the 2D square lattice as obtained from QMC simulations [12]. Shown is the first Mott lobe with filling factor $n = 1$. The arrow indicates the fixed-density transition through the tip of the lobe.

potential μ . Here, ω_p (ω_q) is the energy of photons (qubits). The spin operators σ^\pm describe intrasite transitions between the two qubit levels induced by emission or absorption of a photon with rate g (light-matter coupling). The second term in (1) describes photon transfer between nearest neighbor sites i and j with hopping amplitude t . The polariton density (filling factor) is denoted as $n \equiv \langle \hat{n} \rangle = \langle \hat{N} \rangle / L^2$, where L^2 is the number of lattice sites. We use g as the unit of energy, and consider $\omega_p = \omega_q = 1$ (resonance condition).

Similar to the BHM, the ground-state phase diagram of the JCHM consists of a series of Mott-insulating lobes with integer filling factor n . The extent of the lowest Mott lobe with $n = 1$ for the 2D square lattice considered here is known from QMC simulations [12], see Fig. 1. The generic MI-SF transition in the 2D BHM caused by density fluctuations is known to be of the mean-field type with a dynamical critical exponent $z = 2$ [1, 2]. However, when increasing the hopping t along a path that leads through the tip of the Mott lobe while keeping the polariton density constant, the transition is driven by phase fluctuations. This special case belongs to the universality class of the (2+1)D XY model with $z = 1$ [1, 4]. This means that particle and hole excitations become symmetric near the tip of the lobe and that the critical field theory describing this transition is relativistic with equal scaling of space and time directions. The location of the lobe tip has been determined as $\mu/g = 0.185(5)$, $t_c/g = 0.05201(10)$ [12]. For the 2D JCHM, previous QMC simulations have confirmed $z = 2$ for the generic, density-driven transition. However, the same QMC simulations also suggest that the special $z = 1$ point at the tip of the lobe in the BHM is absent in the JCHM. On the other hand, analytical calculations of the excitation spectra [14, 15] and general symmetry arguments based on the gauge invariance of the theory [13] predict a special point with $z = 1$ at the lobe tip in the JCHM as well.

Method In order to resolve this controversy and to determine the dynamical critical exponent z , we compute the finite-size scaling behavior of the superfluid density ρ_s and the com-

pressibility κ . Scaling relations for both quantities are known from Ref. [1]. The superfluid density is related to fluctuations of the winding number W in QMC simulations via [22]

$$\rho_s = \frac{\langle W^2 \rangle}{\beta D L^{D-2}}. \quad (2)$$

The finite-size scaling form of ρ_s reads

$$\rho_s = L^{2-D-z} \tilde{\rho}_s[(t - t_c)L^{1/\nu}, \beta/L^z], \quad (3)$$

where ν denotes the correlation length exponent. Fixing the ratio $\alpha = \beta/L^z$, the quantity

$$L^{D-2+z} \rho_s[(t - t_c)L^{1/\nu}, \alpha] \quad (4)$$

depends only on the distance from the critical point, $(t - t_c)L^{1/\nu}$, so that at $t = t_c$ curves for different L as a function of t intersect in a single point. This allows to determine the critical value t_c for the MI-SF transition. Plotting $L^{D+z-2} \rho_s$ as a function of $(t - t_c)L^{1/\nu}$ should lead to a scaling collapse of results for different L .

A second observable of interest is the compressibility $\kappa = \partial n / \partial \mu$, which, by the fluctuation-dissipation theorem, can also be expressed in terms of number fluctuations, i.e.,

$$\kappa = \beta (\langle \hat{n}^2 \rangle - \langle \hat{n} \rangle^2), \quad (5)$$

with the scaling form

$$\kappa = L^{z-D} \tilde{\kappa}[(t - t_c)L^{1/\nu}, \alpha] \quad (6)$$

implying that $L^{D-z} \kappa$ should be independent of L at t_c .

For the calculation of ρ_s and κ , the Hamiltonian (1) is simulated using world lines in the stochastic series expansion (SSE) representation [20, 23]. This is the same method as previously used by Zhao et al. [12]. We have used the ALPS 1.3 implementation [23] of the SSE with directed loop updates [24, 25]. In the vicinity of the MI-SF boundary of the first Mott lobe, allowing a maximum of six photons respectively polaritons per site is sufficient to eliminate any noticeable error. We considered $L \times L$ square lattices. The inverse temperature β was chosen as $\beta g = 2L$ for $z = 1$ and $\beta g = L^2/4$ for $z = 2$. We also performed QMC simulations using the worm algorithm [26] in the path integral representation following the implementation of Ref. [27]. No cutoff in the polariton number is needed in this case. The results on up to 64×64 lattices (not shown) are in full agreement with our SSE data.

The conclusion of $z = 2$ scaling for the whole MI-SF phase boundary in previous work was based on results for the superfluid density on lattice sizes up to 22×22 [12]. Here we present data for both the superfluid density and the compressibility, using much larger system sizes up to 40×40 . The existence of a $z = 1$ critical point should also be visible in numerical simulations in a finite range of parameters around the lobe tip [12]. Hence, a grand-canonical algorithm with a suitably chosen chemical potential (here $\mu/g = 0.185$ [12]) can be used, as confirmed by the results below.

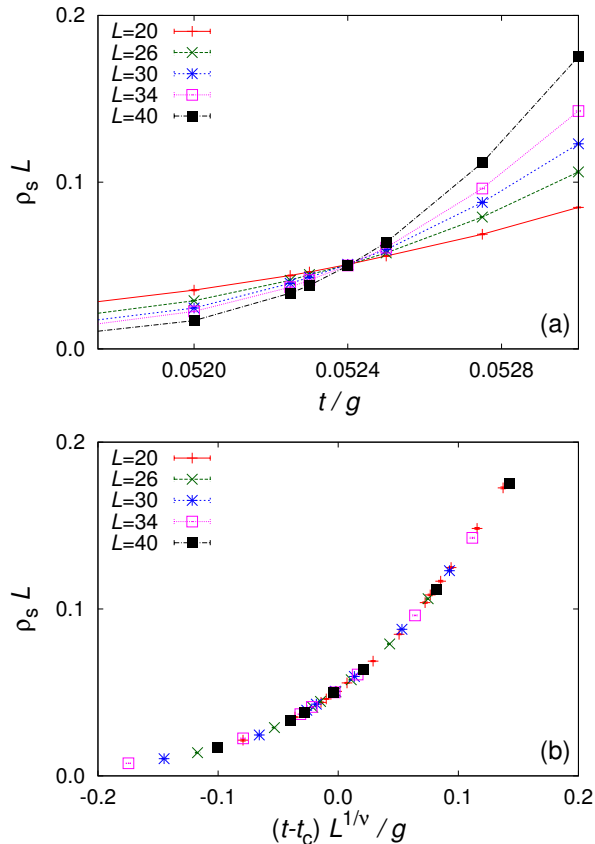


FIG. 2: (Color online) Scaling of the superfluid density ρ_s across the fixed-density transition at $\mu/g = 0.185$ [12] using $L \times L$ square lattices and $\beta g = 2L$. The intersect of $L\rho_s$ for different lattice sizes L in a single point in panel (a) is evidence for a dynamical critical exponent $z = 1$, and defines the critical point at $t_c/g = 0.05242(1)$. (b) Scaling collapse using $t_c/g = 0.05242$ and $\nu = 0.6715$ [4].

Results First, we consider the scaling behavior of ρ_s and κ assuming $z = 1$. In that case fluctuations in space and (imaginary) time are isotropic and the winding number in space (leading to a nonzero superfluid stiffness) scales the same way as the winding number in imaginary time (leading to a nonzero compressibility). Results for $z = 1$ with the aspect ratio $\beta g/L = \text{const.} = 2$ are shown in Figs. 2 and 3.

Figure 2(a) shows the rescaled superfluid density $\rho_s L$ as a function of the hopping strength t/g for system sizes ranging from 20×20 to 40×40 . The intersect of the curves leads to the estimate of the critical hopping strength $t_c/g = 0.05241(1)$. The previous estimate was $t_c/g = 0.05201(10)$ [12]. Our value of t_c , together with the correlation length exponent $\nu = 0.6715$ (as found numerically for the BHM [4]), leads to a clean scaling collapse in Fig. 2(b). We also observe that we need bigger system sizes for the JCHM as compared to the BHM in order to see a clear scaling collapse.

Figure 3 shows a similar analysis for the compressibility κ . The value of t_c from the intersect in Fig. 3(a) coincides within errorbars with the value obtained from the superfluid density.

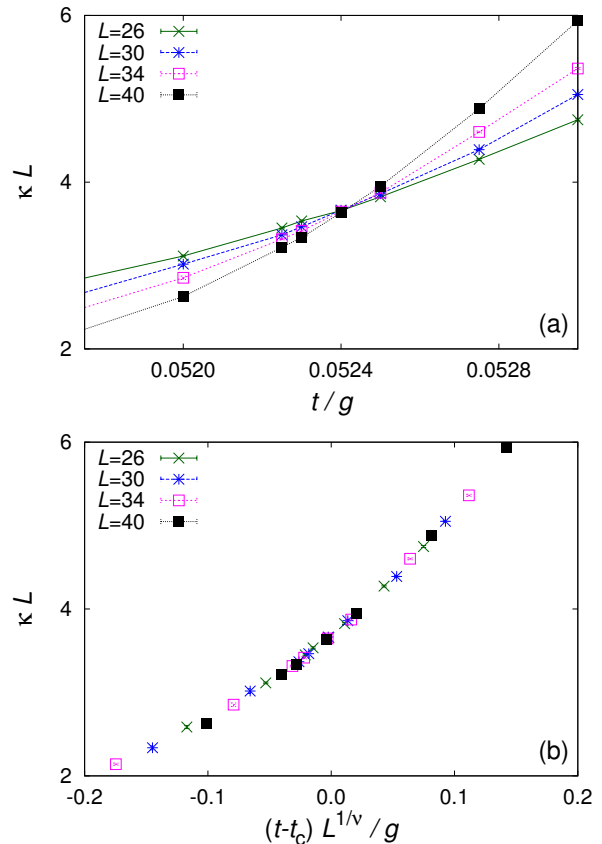


FIG. 3: (Color online) Scaling of the compressibility κ for the same parameters as in Fig. 2. The intersect in (a) is consistent with $z = 1$ and occurs at the same value of the critical hopping strength $t_c/g = 0.05242(1)$ as in Fig. 2. (b) Scaling collapse using $t_c/g = 0.05242$ and $\nu = 0.6715$ [4].

Again, we find a very clean scaling collapse in Fig. 3(b). Our results are thus fully consistent with $z = 1$.

In Ref. [12], an apparent scaling collapse for the superfluid density was found assuming $z = 2$. In Fig. 4 we therefore present our results for the case $z = 2$ with $\beta g/L^2 = \text{const.} = 1/4$. We point out that we do not find any contradiction between our numerical data and those of Ref. [12] when considering the same system sizes. The curves for the superfluid density, shown in the Fig. 4(a), seem to cross in a single point and one may be tempted to think that $z = 2$ applies equally well [12]. However, differences clearly show up for larger system sizes. Figure 4(b) shows finite-size scaling corrections to the critical value of the hopping strength that go as $1/L^2$. The extrapolation of those intersection points yields a critical value for the hopping strength that is within error bars the same as the one found for $z = 1$ scaling. The estimate of t_c for smaller L matches the result of Ref. [12]. These observations can be understood from Eq. (2): The winding number, which is an integer, is in 2D given by $\langle W^2 \rangle \sim \rho_s \beta$, and hence the leading term in the finite size scaling for the superfluid density cannot distinguish between $z = 1$ and $z = 2$. The small

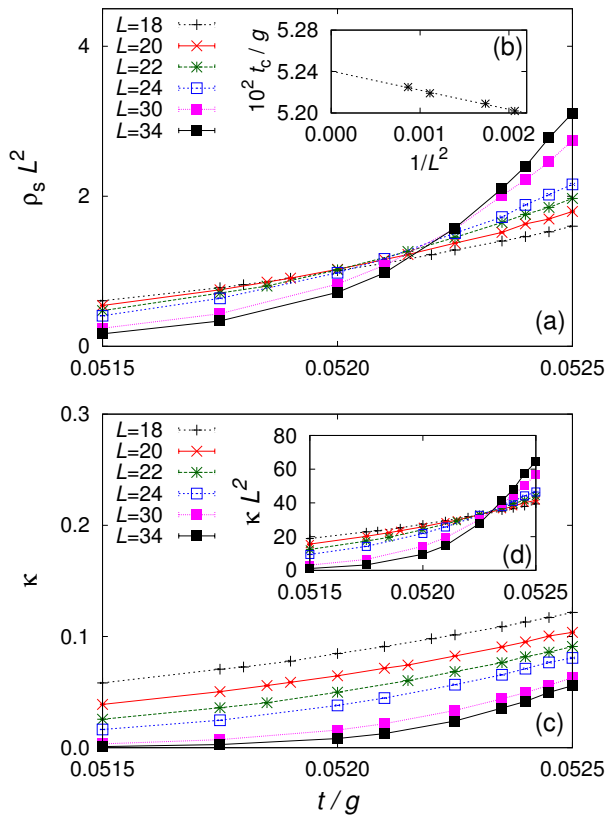


FIG. 4: (Color online) Scaling of the superfluid density ρ_s and compressibility κ across the fixed-density transition at $\mu/g = 0.185$ [12] using $\beta g = L^2/4$. In (a), the intersect of curves for consecutive system sizes [shown in panel (b)] approaches the t_c obtained in Figs. 2 and 3. Panel (c) shows the compressibility for the same parameters, with no intersection in the vicinity of t_c . Panel (d) illustrates the intersect obtained when plotting κL^2 .

subleading corrections we see in Fig. 4(b) (while we were unable to resolve any such drifts in the $z = 1$ scenario within the resolution of our numerical data) therefore provide further evidence that $z = 1$ is correct. Using the full range of system sizes available here, no scaling collapse is achieved assuming $z = 2$.

An even stronger distinction between $z = 1$ and $z = 2$ can be made using results for the compressibility. To this end, we plot in Fig. 4(b) $\kappa L^0 = \kappa$ as appropriate for $z = 2$ —cf. Eq. (6). The absence of a crossing point on the scale of the plot suggests that there are strong corrections to the scaling assumption, making $z = 2$ very unlikely. In contrast, κ scales as expected for the generic transition of the JCHM (not shown).

Finally, if $z = 1$ is correct, relativistic invariance allows us to interpret the imaginary time axis as a spatial axis, and vice versa. Consequently, κL^2 (with $\beta \sim L^2$ scaling) should behave identically to $\rho_s L^2$. This is shown in Fig. 4(d). We therefore conclude that $z = 1$ must be true, and we see no physical reason to investigate other scenarios such as theories with a fractional z .

Summary We have shown on the basis of finite-size scaling of the superfluid density and the compressibility that the fixed-density Mott-insulator-superfluid transition in the 2D Jaynes-Cummings-Hubbard model falls into the 3D XY universality class. The critical behavior is thus identical to the corresponding transition in the Bose-Hubbard model.

Acknowledgments We are grateful to G. Blatter, J. Keeling, K. Le Hur, P. Pippa, N. V. Prokof'ev, and M. Troyer for valuable discussions. MH was supported by the DFG FG1162, and acknowledges the hospitality of ETH Zurich. LP was supported by the Swiss National Science Foundation under Grant No. PZ00P2-131892/1. Part of the simulations were performed on the Brutus cluster at ETH Zurich.

-
- [1] M. P. A. Fisher, P. B. Weichman, G. Grinstein, and D. S. Fisher, Phys. Rev. B **40**, 546 (1989).
 - [2] F. Alet and E. S. Sorensen, Phys. Rev. B **70**, 024513 (2004).
 - [3] N. Elstner and H. Monien, Phys. Rev. B **59**, 12184 (1999).
 - [4] B. Capogrosso-Sansone, S. G. Söyler, N. Prokof'ev, and B. Svistunov, Phys. Rev. A **77**, 015602 (2008).
 - [5] M. Greiner *et al.*, Nature (London) **415**, 39 (2002).
 - [6] J. Kasprzak *et al.*, Nature (London) **443**, 409 (2006).
 - [7] A. D. Greentree, C. Tahan, J. H. Cole, and L. C. L. Hollenberg, Nat. Phys. **2**, 856 (2006).
 - [8] M. J. Hartmann, F. G. S. L. Brandão, and M. B. Plenio, Nat. Phys. **2**, 849 (2006).
 - [9] D. G. Angelakis, M. F. Santos, and S. Bose, Phys. Rev. A **76**, 031805 (2007).
 - [10] M. Aichhorn, M. Hohenadler, C. Tahan, and P. B. Littlewood, Phys. Rev. Lett. **100**, 216401 (2008).
 - [11] D. Rossini and R. Fazio, Phys. Rev. Lett. **99**, 186401 (2007).
 - [12] J. Zhao, A. W. Sandvik, and K. Ueda, arXiv:0806.3603 (2008).
 - [13] J. Koch and K. Le Hur, Phys. Rev. A **80**, 023811 (2009).
 - [14] S. Schmidt and G. Blatter, Phys. Rev. Lett. **103**, 086403 (2009).
 - [15] S. Schmidt and G. Blatter, Phys. Rev. Lett. **104**, 216402 (2010).
 - [16] M. Knap, E. Arrigoni, and W. von der Linden, Phys. Rev. B **82**, 045126 (2010).
 - [17] N. Na, S. Utsunomiya, L. Tian, and Y. Yamamoto, Phys. Rev. A **77**, 031803 (2008).
 - [18] P. A. Ivanov *et al.*, Phys. Rev. A **80**, 060301 (2009).
 - [19] M. Hartmann, F. Brandao, and M. Plenio, Laser & Photonics Review **2**, 527 (2008).
 - [20] P. Pippa, H. G. Evertz, and M. Hohenadler, Phys. Rev. A **80**, 033612 (2009).
 - [21] E. T. Jaynes and F. W. Cummings, Proc. IEEE **51**, 89 (1963).
 - [22] E. L. Pollock and D. M. Ceperley, Phys. Rev. B **36**, 8343 (1987).
 - [23] A. Albuquerque *et al.*, J. Magn. Magn. Mater. **310**, 1187 (2007).
 - [24] O. F. Syljuåsen and A. W. Sandvik, Phys. Rev. E **66**, 046701 (2002).
 - [25] F. Alet, S. Wessel, and M. Troyer, Phys. Rev. E **71**, 036706 (2005).
 - [26] N. V. Prokof'ev, B. V. Svistunov, and I. S. Tupitsyn, J. Exp. Theor. Phys. **87**, 310 (1998).
 - [27] L. Pollet, K. Van Houcke, and S. M. A. Rombouts, J. Comput. Phys. **225**, 2249 (2007).